Korean J. Chem. Eng., **26**(1), 175-181 (2009)

Kinetics of nucleation and growth of L-sorbose crystals in a continuous MSMPR crystallizer with draft tube: Size-independent growth model approach

Bogusława Wierzbowska*, Krzysztof Piotrowski,†, Joanna Koralewska*, Nina Hutnik*, and Andrzej Matynia***

*Faculty of Chemistry, Wroclaw University of Technology, Wybrzeze Wyspianskiego 27, 50-370 Wroclaw, Poland
**Department of Chemical and Process Engineering, Silesian University of Technology,
ks. M. Strzody 7, 44-101 Gliwice, Poland
(*Received 3 April 2008 • accepted 3 August 2008*)

Abstract−The experimental data concerning kinetics of a continuous mass crystallization in L-sorbose - water system are presented and discussed. Influences of L-sorbose concentration in a feeding solution and mean residence time of suspension in a working volume of laboratory DT MSMPR crystallizer on the resulting crystal size distributions, thus on the nucleation and growth kinetics, were determined. The kinetic parameter values were evaluated on the basis of size-independent growth (SIG) kinetic model (McCabe's ΔL law). It was observed that within the investigated range of crystallizer productivity (220-2,200 kg of L-sorbose crystals m^{-3} h^{-1}), a crystal product of mean size L_m from 0.22 to 0.28 mm and CV from 68.8 to 44.0% was withdrawn. The values of linear growth rate show increasing trend (from $6.6 \cdot 10^{-8}$ to $7.6 \cdot 10^{-8}$ m s^{-1}) with the productivity enlargement (assuming constant residence time τ=900 s). Occurrence of secondary nucleation phenomena within the circulated suspension, resulting from the crystals attrition and breakage was observed. The parameter values in a design equation, matching linear growth rate and suspension density with nucleation rate were determined.

Key words: L-Sorbose, Continuous Mass Crystallization, Water Solution, Draft Tube (DT) Crystallizer, Size-independent Growth (SIG) Kinetic Model

INTRODUCTION

L-sorbose ($C_6H_{12}O_6$, molar mass 180.16 kg $kmol^{-1}$) is a crystalline substance (temperature of melting point 438 K, density 1,650 kg m^{-3}), of white color and sweet taste, laevorotatory ($[\alpha_D^{30}]=-42.7^o$), crystallizing in a rhombic system (bisphenoidal crystals). It is a substance easily soluble in water [1,2], however only slightly soluble in alcohols. This monosaccharide is an intermediate product in L(+)-ascorbic acid (vitamin C) synthesis technology according to the Reichstein procedure [3-5]. It is formed as a result of biochemical dehydrogenation of D-sorbitol by *Gluconobacter* (*Acetobacter*) *suboxydans* [6-8]. As an intermediate product it must satisfy the following requirements: appearance of light-yellow or colorless crystals, maximal moisture content: 0.2 mass% and main component content: 97-98.8 mass%. Technical grade L-sorbose synthesized under industrial conditions is a subject of purification, the most frequent by multistage, consecutive batch mass crystallization from their water solutions. This process, however, involves a relatively large number of labor-consuming operations, that favors decomposition of L-sorbose, thus deteriorates the product crystals quality [1,9].

One of the important problems in this technology is that water solutions of L-sorbose tend to form stable supersaturated systems of high values of maximal supercooling: from about 10 up to about 50 K, depending on saturation temperature of the feed solution, as well as on the cooling rate applied [2,10,11]. Both process parameters influence nucleation and crystal growth kinetics significantly [10], determining the process yield and product quality (crystal size distribution, their uniformity, shape and chemical purity) [12]. To improve the process efficiency and to raise the solid product quality there are also attempts of introducing a third compound into the original binary crystallizing system - methanol or/and ethanol [13-15]. In the accessible literature there are no reports concerning the application of a continuous regime for mass crystallization of L-sorbose. This situation results, among other things, from the fact that the principal process of vitamin C synthesis, with the use of L-sorbose as an intermediate product, is from technical reasons the most often realized in a batch mode. However, experimental determination of the basic kinetic parameters corresponding to an alternative, continuous mode of operation seems to be advisable. Especially beneficial can be practical utilization of the mentioned earlier, large metastable zone width, desirable in a continuous regime (stable conditions of crystals growth, confined primary nucleation), in contradistinction to a batch mode (difficulties in the crystal phase appearing within a closed system). The test results can be recognized as valuable, comparative material for the analysis of both continuous and batch variants in L-sorbose purification technology.

The experimental results concerning the kinetics of continuous mass crystallization of L-sorbose from its water solutions are thus presented and discussed. A simplified kinetic model of MSMPR crystallizer, assuming size-independent growth mechanism (G(L)= G=const., SIG kinetic model) was used for the kinetic data evaluation.

EXPERIMENTAL

1. Laboratory Setup

A connection scheme of a laboratory stand is presented in Fig. 1. The experimental plant was composed of devices made by IKA

†To whom correspondence should be addressed.
E-mail: krzysztof.piotrowski@polsl.pl

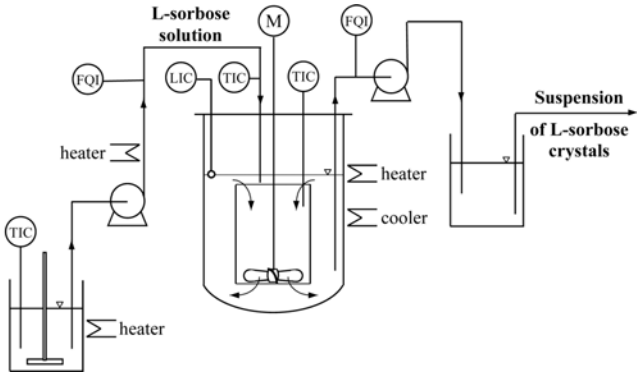

Fig. 1. Experimental setup of a laboratory continuous DT MSMPR crystallizer.

Labortechnik, Germany. Operating and control was provided by PC computer driven by professional IKA Labworldsoft software.

The tests were carried out in a laboratory-scale continuous DT MSMPR (*Draft Tube*, *Mixed Suspension Mixed Product Removal*) crystallizer with internal circulation of suspension (modified IKA laboratory reactor system LR-A1000). It was a hermetic, glass-made cylindrical tank (V_t=1 dm^3, D=120 mm, H=123 mm), inside which a circulation tube was fixed (*Draft Tube*, DT, d=61 mm, h=53 mm). In the tank axis, inside the circulation profile, a three-paddle propeller mixer (d_m=55 mm) was installed. In all experiments the revolution number was kept constant (N=10±0.2 s^{-1}), resulting in stable and intensive enough circulation of suspension inside the crystallizer working volume (V_w=0.6±0.02 dm^3). The bottom section of the crystallizer vessel was provided with a heating/cooling jacket integrated with externally circulated distilled water of adjustable temperature. It assured constant temperature of suspension inside the crystallizer vessel, T_{cr}=293 K, with the accuracy of ±0.2 K. The arrangement of heating/cooling systems and spatial distribution of control/regulation points of temperature (TIC), flow rate (FQI), suspension level (LIC) and stirrer revolution number (M) are indicated in Fig. 1. The solutions tested, as biochemically active systems, were prepared just before their introduction into the crystallizer by using analytically pure L-sorbose of the main component content ≥98 mass% (suitable for biotechnological purposes, SAFC FLUKA, Germany) and double distilled water. Temperature T_{rm} in a feeding solution reservoir (see Fig. 1) was about 10 K higher than the saturation temperature T_{eq} of a feeding solution (individually selected for its current chemical composition). Moreover, the delivery pipe of the feeding solution (see Fig. 1) was insulated and heated. This technical arrangement prevented the undesirable, spontaneous nucleation within the feeding solution before its introduction into the process environment. All elements of the crystallizer and installation contacting with L-sorbose solution or crystal suspension were made with chemically inactive glass or plastic, while the mixer paddles were covered with protective coating.

2. Test Scope

The effect of concentration of L-sorbose in a feeding solution (55-70 mass% of L-sorbose) and mean residence time of suspension in a crystallizer working volume (900-3,600 s) on product crystal size distribution was tested. Two test series were carried out. In the first set of experiments, the concentration of L-sorbose in a feeding solution was: 55 (T_{eq}=324.5 K), 60 (T_{eq}=339.0 K), 65 (T_{eq}=353.5 K) and 70 (T_{eq}=368.0 K) while a constant suspension residence time, τ=900 s, was assumed. In the second series, a constant concentration of L-sorbose was assumed (55 or 65 mass%) while the values of mean residence time were elongated up to 1,800 and 3,600 s, respectively. The tested parameter ranges were selected taking under consideration some special technological requirements of a continuous mass crystallization of L-sorbose ($[LS]_{rm}$, T_{rm}) [2,10,12], as well as the technical ability of controlling the process course under the laboratory conditions (T_{cr}, τ). Solubility of L-sorbose in water ($[LS]_{eq}$=f(T)) and density of its saturated water solutions (ρ_{sat}=f(T)) are presented in [1,2].

3. Test Procedure

The individual measurement procedure was as follows. Working volume of the crystallizer was filled with initial suspension of L-sorbose crystals. Then, simultaneously, the tank was fed with a fresh solution and the product crystal suspension was removed. Volumetric flow rate of feeding solution resulted from the assumed mean residence time of suspension. After stabilization of the process parameters (T_{cr}=293 K, V_w=0.6 dm^3, N=10 s^{-1}), the continuous mass crystallization of L-sorbose was running through the time of t=7τ. The whole final suspension was then removed from the tank and mechanically separated from the post-processed mother solution in a centrifuge. The crystals were subsequently washed with water and ethanol solution, respectively, dried in the darkness and finally weighed. Residual concentration of L-sorbose in the mother solution (thus undischarged supersaturation) was determined with the weight method based on the total evaporation of a solvent from the liquid sample of solution.

Crystal size distribution of L-sorbose product was determined with the use of a particle laser analyzer COULTER LS-230. Individual population density values, n_i, were calculated from the experimental mass m(L) or volume V(L) size distribution data according to the formula presented below, Eq. (1):

$$n_i = \frac{m_i}{k_v \rho L_i^3 \Delta L_i V_w} = \frac{V_i}{k_v L_i^3 \Delta L_i V_w} \tag{1}$$

4. Size-Independent Growth (SIG) Model Assumptions - Design Equation of MSMPR Crystallizer

Theoretical assumptions of a continuous MSMPR crystallizer model were accepted: steady state mode, ideally mixed working volume (thus the product sample is identical in size distribution and mother liquor composition to the crystallizer's content), excluding of breakage and agglomeration of particles, all nuclei are formed at zero size and shape similarity within all crystals is observed (their size may be thus characterized by one dimension, L, only). Under these assumptions the general population balance equation reduces to [16]:

$$\frac{d[G(L)n(L)]}{dL} + \frac{n(L)}{\tau} = 0 \tag{2}$$

Moreover, assuming that the crystal growth kinetics meets the McCabe's rule (for a given supersaturation linear growth rate is a constant value for the whole population, size-independent growth (SIG) kinetics):

$$G(L)=G=\text{const.} \tag{3}$$

Eq. (2) can be presented as:

$$G\frac{dn(L)}{dL}+\frac{n(L)}{\tau}=0 \tag{4}$$

Solving Eq. (4) with respect to n(L) results in the derivation of a following function of population density distribution in MSMPR crystallizer:

$$n(L)=n_0\exp\left(-\frac{L}{G\tau}\right) \tag{5}$$

Eq. (5) enables one to determine the basic kinetic parameters of the mass crystallization process: nucleation and growth rates. The plot of lnn versus L should give a straight line with an intercept at L=0 equals to n_0 and a slope corresponding to $-1/G\tau$. If the suspension residence time, τ, is known, the linear growth rate, G, can be calculated directly. Finally, from the nuclei population density, n_0, and linear growth rate, G, values nucleation rate B can be calculated, Eq. (6):

$$B=n_0G \tag{6}$$

as well as specific surface area of suspension, A_T, and suspension density, M_T:

$$A_T=2k_a n_0(G\tau)^3 \tag{7}$$

$$M_T=6k_v\rho n_0(G\tau)^4 \tag{8}$$

Some parameters characterizing crystal size distribution of MSMPR apparatus product can be determined, as well:

$$L_m=4G\tau \tag{9}$$

$$L_{50}=3.67G\tau \tag{10}$$

The values of L_m and L_{50}, Eqs. (9) and (10), depend not only on the linear growth rate, G, and on the mean residence time of suspension, τ, but also, indirectly, on the nucleation rate, B. Influence of Δc, resulting from the simultaneous interactions between nucleation and crystal growth processes, depending on the surface area developed by crystal population in a crystallizer (A_T) at its selected productability (M_T/τ), is represented indirectly by a G value. For the design calculations some empirical equations of the following general form are usually used [17,18]:

$$B=k_N(\Delta c)^n \qquad n>g \tag{11}$$

$$G=k_G(\Delta c)^g \qquad 1<g<2 \tag{12}$$

Eqs. (11) and (12) can be also integrated into one equation:

$$B=k_{NG}G^i \tag{13}$$

where parameter i (*coefficient of sensitivity of nucleation with respect to crystal growth*) is defined as:

$$i=\frac{n}{g} \tag{14}$$

A combination of mass and population balances (resulting for the idealized MSMPR crystallizer with SIG kinetics in a relatively simple Eq. (8)) enables one to anticipate the effects of the decisive parameter ($G=f(\Delta c)$, τ) changes as far as concerned the size distribution of product crystals population is concerned. In an effectively mixed crystal suspension, secondary contact nucleation predominates. Its kinetics for the design purposes can be presented in the form of:

$$B=k_{BG}G^iM_T^jN^k \tag{15}$$

or

$$n_0=\frac{B}{G}=(k_{BG}N^k)G^{i-1}M_T^j \tag{16}$$

The design equations, Eq. (15) or (16), specify the technological parameters affecting the size distribution of the product crystals (L_m, L_{50}). For N=const. and T_{cr}=const. (thus k_{BG}=const.) these are: crystal linear growth rate, G, and concentration of crystal phase in a suspension (suspension density), M_T, identified in practice with working supersaturation in a crystallizer [17,18].

RESULTS AND DISCUSSION

In Table 1 there are presented the values of decisive ($[LS]_{rm}$, τ) and the resulting (Δc_{max}, Δc_{ml}, M_T, L_m, L_{50}, CV) parameters of a continuous mass crystallization process of L-sorbose from its water solutions carried out in a laboratory DT MSMPR crystallizer. It was observed that feeding the reactor, working in a steady state regime,

Table 1. Mass crystallization of L-sorbose in a continuous DT MSMPR crystallizer - the process conditions and size characteristics of the resulting products

No.	$[LS]_{rm}$ (mass%)	τ (s)	Δc_{max} (mass%)	Δc_{ml} (mass%)	M_T (kg m^{-3})	L_m (mm)	L_{50} (mm)	CV (%)
1	55	900	10.2	2.0	191	0.224	0.216	62.2
2	60	900	15.2	2.4	308	0.230	0.220	58.2
3	65	900	20.2	3.0	430	0.258	0.257	44.0
4	70	900	25.2	4.1	551	0.245	0.243	48.7
5	55	1,800	10.2	1.2	207	0.230	0.222	66.2
6	55	3,600	10.2	0.6	219	0.265	0.262	68.8
7	65	1,800	20.2	1.8	450	0.268	0.265	52.4
8	65	3,600	20.2	0.9	464	0.280	0.278	56.3

$\Delta c_{max}=[LS]_{rm}-[LS]_{eq,\ Tcr}$

$\Delta c_{ml}=[LS]_{ml,\ Tcr}-[LS]_{eq,\ Tcr}$

Process temperature in a DT MSMPR crystallizer: T_{cr}=293±0.2 K

$[LS]_{eq}$=44.8 mass% in T_{cr}=293 K [2]

with L-sorbose solution of concentration ranging from 55 to 70 mass% (T_{eq}=324.5→368.0 K), the concentration of crystal phase in suspension, M_T, increases from 191 to 551 kg of L-sorbose crystals m^{-3} (for τ=900 s). It corresponds to the crystallizer productivity range between 764 and 2,204 kg of L-sorbose crystals from 1 m^3 of the apparatus working volume per hour.

Mean size of the product crystals, L_m, shows ascending tendency: from about 0.22 to about 0.25 mm, whereas clear increase in the homogeneity of population is observed (CV values decrease significantly from about 62 to 44-49%).

Working supersaturation value in the mother liquor, Δc_{ml}, increases with the increase of L-sorbose concentration in a feeding solution (thus with its saturation temperature increase) from 2.0 to 4.1 mass%. These supersaturation values are relatively high. It can be expected that the increase in Δc_{ml} results mainly from two important reasons. Nearly 2.5-times increase in a maximal supersaturation value appearing in a feed point of crystallizer (Δc_{max}=10.2→25.2 mass%, see Table 1) requires longer residence time for its efficient blending with the circulated magma to discharge. Thus, the assumed mean residence time τ=900 s (constant in the experiments No. 1-4, Table 1) seems to be too short in respect to the process kinetics requirements. However, its elongation up to 3,600 s results in a noticeable decrease in the supersaturation Δc_{ml} value down to 0.6 and 0.9 mass% for $[LS]_{rm}$=55 and 65 mass%, respectively (experiments No. 6 and 8, Table 1). Secondly, nearly 3-times increase in the concentration of crystal phase in suspension, M_T, is observed, which - assuming constant mixer revolution number in all experiments (N=10 s^{-1}), thus supplying the system with a constant mixing power regardless of the current magma characteristics - results in a decrease in intensity of suspension circulation. Under these conditions the supersaturation discharge rate decreases.

With the elongation of mean residence time (from 900 to 3,600 s) an increase (by 8-15%) in concentration of crystals in suspension, M_T, was reported. It results from over 3-times decrease in a supersaturation value in mother liquor, Δc_{ml}. Nevertheless, with the elongation of mean residence time the crystallizer's productivity decreases from 764 (τ=900 s) to 219 kg of L-sorbose crystals m^{-3} h^{-1} (τ=3,600 s), assuming constant composition of feeding solution ($[LS]_{rm}$=55 mass%). For other composition, $[LS]_{rm}$=65 mass%, it is: 1,720 (τ=900 s)→464 kg of L-sorbose crystals m^{-3} h^{-1} (τ=3,600 s). With the elongation of mean residence time the mean crystal size, L_m, slightly increases from about 0.22 to 0.26 mm (for $[LS]_{rm}$=55 mass%) and from 0.26 to 0.28 mm (for $[LS]_{rm}$=65 mass%). The observed trends in an L_{50} parameter change are qualitatively similar. However, homogeneity in the crystal population decreases: CV=62.2→68.8% ($[LS]_{rm}$=55 mass%) and, more clearly, CV=44.0→56.3% ($[LS]_{rm}$=65 mass%), which results from longer exposition of the circulated/mixed suspension on the attrition/breakage action. It should be noticed that the observed deviations from an ideal MSMPR crystallizer (for which CV=50%) are not significant. It can be thus assumed that the hydrodynamic regime established inside a laboratory crystallizer unit is sufficient enough to, at least roughly, satisfy the theoretical requirements of an ideal MSMPR configuration.

In Fig. 2 there are presented two exemplary experimental population density distributions (Eq. (1)) of L-sorbose crystals corresponding to $[LS]_{rm}$=55 and 65 mass% and mean residence time of suspension τ=900 s (No. 1 and 3 in Table 1). Fig. 3 shows the micro-

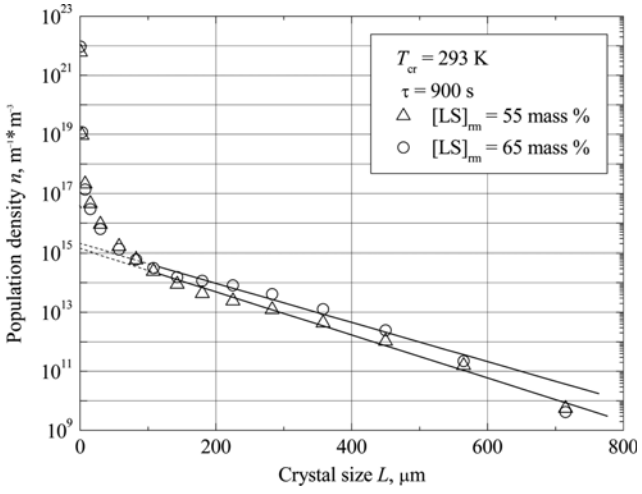

Fig. 2. Comparison of population density distributions of L-sorbose crystals produced in a continuous DT MSMPR crystallizer: the symbols - experimental data, solid lines - the courses calculated with the use of equation 5 valid for the crystals of size L>100 μm (SIG kinetic model applied).

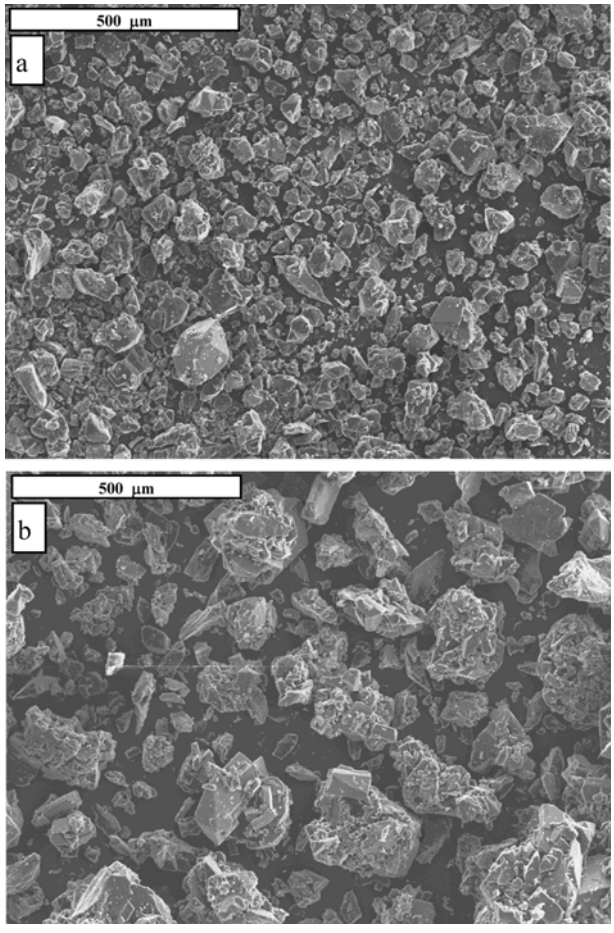

Fig. 3. Scanning microscope images (magnification: 100×) of L-sorbose crystals formed in a continuous DT MSMPR crystallizer: (a) test No. 1, (b) test No. 4 - see the corresponding data in Tables 1, 2 and in Fig. 2.

Table 2. The values of nucleation rate and crystal linear growth rate observed in L-sorbose-water system at T=293 K. Size-Independent Growth (SIG) kinetic model applied

Feeding solution (see Table 1)	τ(s)	Detailed n(L) form (valid for L>100 μm)	R^2	$n_0 \cdot 10^{-15}$ ($m^{-1}m^{-3}$)	$G \cdot 10^{8}$ ($m\ s^{-1}$)	$B \cdot 10^{-7}$ ($m^{-3}s^{-1}$)
1	900	$1.39 \cdot 10^{15} \exp(-1.68 \cdot 10^{4} L)$	0.989	1.39	6.61	9.19
2	900	$1.95 \cdot 10^{15} \exp(-1.59 \cdot 10^{4} L)$	0.993	1.95	6.99	13.60
3	900	$2.02 \cdot 10^{15} \exp(-1.53 \cdot 10^{4} L)$	0.983	2.02	7.26	14.66
4	900	$2.48 \cdot 10^{15} \exp(-1.46 \cdot 10^{4} L)$	0.991	2.48	7.61	18.87
5	1,800	$1.17 \cdot 10^{15} \exp(-1.63 \cdot 10^{4} L)$	0.993	1.17	3.41	3.99
6	3,600	$0.98 \cdot 10^{15} \exp(-1.47 \cdot 10^{4} L)$	0.990	0.98	1.89	1.85
7	1,800	$1.75 \cdot 10^{15} \exp(-1.46 \cdot 10^{4} L)$	0.987	1.75	3.81	6.67
8	3,600	$1.46 \cdot 10^{15} \exp(-1.40 \cdot 10^{4} L)$	0.989	1.46	1.98	2.89

for k_v=1

scope images (scanning electron microscope JEOL-5800 LV) of these crystals. From the courses of population density distribution of L-sorbose crystals, presented in an lnn–L coordinate system (Fig. 2) it results that for the particles of size L>100 μm this dependency can be approximated by a straight line. This enables one to estimate the linear growth rate of crystals, G, as well as nucleation rate, B, from the assumed SIG MSMPR kinetic model, Eqs. (5)-(6) (see Table 2 for the results).

From Fig. 2 it is also seen that in an lnn−L coordinate system for the crystals of size L<100 μm the experimentally determined population density distributions are concave to the top. This characteristic shape can be interpreted theoretically as evidence of a more complex intrinsic kinetics of the crystal phase growth than it can result from the most simplified SIG model. In particular, this type of population density distribution can result from the occurrence of size-dependent phenomena causing diversification in the convective mass transfer resistances (G(L)≠const., SDG) or/and growth rate dispersion (G_i=const., GRD), as well as secondary nucleation contribution. It should be noticed, that both kinetic phenomena (SDG and GRD) are undistinguishable considering the population density distribution data only; thus for engineering calculation purposes can be treated as integrity (since both produce identical external effect) and be a subject of description by a more mathematically convenient SDG model. Alternative description of the mass crystallization process of L-sorbose with the use of a more complex SDG kinetic model will be presented in the authors' next work.

From a detailed analysis of scanning microscope images of crystal product (see Fig. 3) it results that the main process of mass crystallization of L-sorbose is accompanied by agglomeration and secondary nucleation. Conglomerated small particles are observed, while some of the larger crystals demonstrate surface defects and rounded edges. Some disrupted fragments of larger parent crystals are present, as well. From the corresponding population density distributions (see Fig. 2) it results that attrition/breakage effects are partly compensated by agglomeration of newly born fragments, which, together with the potential occurrence of GRD and size-dependent hydrodynamic phenomena in mass transfer processes, results in a concave shape of an lnn(L) function within the smallest crystal size range.

In Table 2 there are presented the detailed forms of Eq. (5), the population density distributions of L-sorbose crystals produced in the assumed process/hydrodynamic conditions, valid for L>100 μm, as well as calculated on these basis values of kinetic parameters (n_0, G, B). Increase in L-sorbose concentration in a feeding solution (thus increment in M_T value in a crystallizer vessel) for a constant mean residence time τ=900 s produces an increase in the linear growth rate of crystals, G: from about $6.6 \cdot 10^{-8}$ up to about $7.6 \cdot 10^{-8}$ m s^{-1}. However, the nucleation rate, B, simultaneously increases more than 2-times. Elongation in mean residence time of suspension in a crystallizer working volume τ=900→3,600 s, irrespective of L-sorbose concentration in a feeding solution (55 or 65 mass%), results in a decrease in both kinetic parameter values: about 3.5-times decrease in the linear growth rate value, G, and about 5-times decrease in the nucleation rate, B. Consequently, the mean product size increases by about 20% ($[LS]_{rm}$=55 mass%) and by about 8% ($[LS]_{rm}$=65 mass%) (see Table 1).

Application of nonlinear regression methods to the experimental data, M_T, G and B (Tables 1 and 2), enables one to calculate the exponent values in Eq. (15) or (16). For T_{cr}=const.=293±0.2 K and N=const.=10±0.2 s^{-1} these are i=1.34, j=0.48. Eq. (15) can be thus presented in detailed form:

$$B = 3.14 \cdot 10^{16} G^{1.34} M_T^{0.48} \qquad R^2 = 0.981 \tag{17}$$

Generally, in mass crystallization processes: 0.5<i<3 (usually i>1) and 0.4<j<2 (usually j=1) [17,18].

On the basis of exponent values in Eq. (17) one can draw some theoretical conclusions as far as the predominant collision type is concerned in the processes of crystal attrition and breakage, as well as which stage of contact nucleation can be regarded as a limiting factor in this process [18]. For j=0.48<1 and i=1.34>1 (see Eq. (17)) it can be supposed that in the presented conditions L-sorbose nucleation is governed by the process of forming of the potential nuclei on the crystal phase surface. Their integration with the parent crystal surface dominates over their removal (surface regeneration limited kinetics).

Taking into consideration the theoretical assumptions of SIG MSMPR model, the kinetic results can be generally commented as follows:

1. Influence of L-Sorbose Concentration in a Feeding Solution (Influence of Suspension Density M_T)

Increase in an M_T value, as a result of an increase in the feeding solution concentration $[LS]_{rm}$, for T_{cr}=const., N=const., τ=const. and j=1 theoretically should result in (according to SIG kinetic model

predictions, Eq. (8) and Eqs. (11)-(16)) the constant values of L_m, G and Δc_{ml}. From the experimental data analysis it can be concluded that these are not. Mean crystal size of L-sorbose, L_m, and its linear growth rate, G, increase (tests No. 1-No. 4, Tables 1 and 2), while exponent j=0.48≠1 (Eq. (17)). The main reason for this observation is, first, an increase in the working supersaturation Δc_{ml} value (more than 2-times), in spite of the increase in the specific surface area of the crystals, A_T (Eq. (7)), resulting from higher concentration of the crystals in suspension, M_T, thus a more intensive attrition action. Larger specific surface area of crystal phase should theoretically correspond to a lower working supersaturation level, since in this process environment mass transfer resistances can be effectively reduced. However, unexpected and significant increase in a working supersaturation value was observed, which, as it was mentioned above, resulted most likely from relatively high local values of maximal supersaturation at the feeding solution's inlet Δc_{max}, as well as from too short mean residence time, τ, and constant (thus not appropriately adjusted if necessary) mixer's revolution number, N; both produced ineffective supersaturation distribution within the bulk mother solution.

Increase in concentration of crystal phase in suspension (suspension density, M_T) is advantageous from economical reasons, since the crystallizer productivity can be increased. Nevertheless, in practice, as was already emphasized, these conditions are accompanied by the increase in intensity of crystal attrition and breakage, which, in turn, influences mean product size disadvantageously. About 15% increase in linear growth rate of crystals was reported while nucleation rate increased more than 2-times. Mean crystal size increased by about 10%.

2. Influence of Mean Residence Time, τ

From the SIG model it can be concluded that for i>1 elongation in mean residence time, τ, assuming T_{cr}=const., M_T=const. and N=const., should produce a decrease in linear growth rate, G, value (Eq. (8)), increase in mean crystal size, L_m (the effect is more pronounced when i is larger than 1, Eq. (9)) and decrease in a working supersaturation Δc_{ml} value (Eq. (12)). The experimental data (for i=1.34, Eq. (17)) confirm these theoretical predictions (No. 1, 5, 6 and 3, 7, 8, Tables 1 and 2). It is known, however, that in a real crystallizer crystal attrition and breakage occur. Secondary nucleation rate decreases generally with the elongation of mean residence time (Eq. (15)). However, the mechanical disintegration rate alone remains constant (as dependent, among others, on the mixing power). An additional decrease in supersaturation resulted from the increase in a specific surface area of crystal phase, A_T, after disintegration is thus observed, which unfavorably reduces the crystal growth rate value. Working supersaturation value decreased also as a result of M_T value increase (by 8-15% - see Table 1). The $M_T(\tau)$ value was thus not constant, which is an additional, however small, deviation from the theoretical assumptions of the SIG MSMPR kinetic model. Taking under consideration the crystal product quality (L_m, L_{50}, CV), excessive elongation in mean residence time can provide the opposite results than the theoretically expected ones. However, from the laboratory experiments one can see that the maximal mean residence time of suspension in the crystallizer working volume tested, τ= 3,600 s, did not cause any significant negative consequences (see Table 1). Mean crystal size and their homogeneity in the examined process conditions can be regarded satisfactory.

CONCLUSIONS

The continuous mode of mass crystallization of L-sorbose, a raw material for vitamin C synthesis, was presented and discussed. The experiments covered the influence of L-sorbose concentration in a feeding solution ($[LS]_{rm}$=55-70 mass% for τ=900 s), as well as the influence of mean residence time of suspension in a crystallizer working volume (τ=900-3,600 s for $[LS]_{rm}$=55 and 65 mass%) on the process conditions (Δc_{max}, Δc_{ml}, M_T, B, G) and the resulting product properties (L_m, L_{50}, CV).

Increase in solute concentration in a feeding stream $[LS]_{rm}$=55→70 mass% (for τ= 900 s) results in a slight increase in the linear growth rate, G, value from $6.61\cdot10^{-8}$ to $7.61\cdot10^{-8}$ m s^{-1}, whereas elongation in mean residence time, τ=900→3,600 s, produces a visible decrease in the G value: $6.61\cdot10^{-8}$→$1.89\cdot10^{-8}$ m s^{-1} (for $[LS]_{rm}$=55 mass%) and $7.26\cdot10^{-8}$→$1.98\cdot10^{-8}$ m s^{-1} (for $[LS]_{rm}$=65 mass%), respectively.

Since in the literature there is no technological data concerning the continuous regime in the mass crystallization of L-sorbose, one can only compare the kinetic data obtained with the ones corresponding to the batch mode. In [10] it is reported that an increase in the cooling rate (reduction in batch crystallization time, thus a rough counterpart of the mean residence time decrease in the continuous mode case) from $1.39\cdot10^{-3}$ up to $8.33\cdot10^{-3}$ K s^{-1} produces an increase in a linear growth rate of crystals, G, from $0.4\cdot10^{-8}$ m s^{-1} up to $3.5\cdot10^{-8}$ m s^{-1} ($[LS]_{rm}$=55 mass%) and from $0.3\cdot10^{-8}$ m s^{-1} up to $2\cdot10^{-8}$ m s^{-1} ($[LS]_{rm}$=61.5 mass%). In the continuous mode, for comparable compositions of a feeding solution ($[LS]_{rm}$=55 and 65 mass%), these increases are considerably larger, however of the same magnitude. This difference results mainly from the different experimental conditions (pure continuous regime compared with the periodical, polythermic process of nucleation combined with crystal growth). Batch crystallization time was in the range of 0.55-1.80 h, whereas in a continuous mode it was τ=0.15-1 h, which also contributed complex kinetics of the supersaturation discharge. Critical supersaturation in the batch experiments was 8.2-6.0 mass%, while in the continuous mode at the feeding point Δc_{max} attained values as high as 10.2-25.2 mass% (theoretically, the upper metastable zone limit could thus be exceeded). This can be partly responsible for the fact that mean crystal size obtained in the batch regime was considerably larger, L_m=0.28-0.51 mm, whereas in the continuous regime it was 0.22-0.28 mm only. Moreover, in the batch conditions the coefficient of variation CV=51.7-45.2%, while in the continuous regime CV=68.8-44.0 was observed (larger spread within the crystal sizes). With the increase in saturation temperature (thus concentration) linear growth rate of crystals in the batch conditions decreased from about G=$10\cdot10^{-8}$ m s^{-1} down to G≈$2\cdot10^{-8}$ m s^{-1} for the solution of initial concentration of L-sorbose higher than 60 mass% (T_{eq}> 340 K, assuming a linear cooling rate R_T=$8.33\cdot10^{-3}$ K s^{-1}). However, in the continuous process regime a slightly increasing trend was observed: from $6.61\cdot10^{-8}$ m s^{-1} ($[LS]_{rm}$=55 mass%) to $7.61\cdot10^{-8}$ m s^{-1} ($[LS]_{rm}$=70 mass%), assuming τ=900 s (the lowest value of mean residence time can roughly correspond to the highest cooling rate tested).

It should be emphasized, that both batch and continuous experiments were carried out in the same laboratory crystallizer of 0.6 dm^3 working volume, which enables one to assume identity in size,

internal arrangement and resulting hydrodynamic profiles, thus excluding these factors from the kinetic analysis. The only difference was the work regime, batch or continuous, connected with the appropriate laboratory stand arrangement.

The experimental results and elaborated kinetic data can be useful in design and theoretical works, as well as a reference material helpful in examining the feasibility and economical parameters of various technological variants of mass crystallization of L-sorbose from its binary water solutions.

ACKNOWLEDGMENTS

This work was supported by the Scientific Research Committee (Ministry of Science and Higher Education) of Poland under grant No. 3T09B 122 27. The L-sorbose crystal size distributions were measured by means of particle size analyzer COULTER LS-230 at the Institute of Inorganic Chemistry, Gliwice, Poland. The images of L-sorbose crystals (scanning microscope JEOL-5800 LV) were made at the Head of Materials Science Laboratory of the Institute of Materials Science and Applied Mechanics, Wroclaw University of Technology, Wroclaw, Poland.

NOMENCLATURE

A_T : specific surface area of suspension [m^2 m^{-3}]
B : nucleation rate [m^{-3} s^{-1}]
c : concentration [mass%]
Δc : supersaturation [mass%]
CV : coefficient of variation (of crystal sizes) [%]
d : draft tube's diameter [m]
d_m : agitator's diameter [m]
D : crystallizer's diameter (inner) [m]
G : linear growth rate of crystals [m s^{-1}]
h : draft tube's height [m]
H : crystallizer's height (total) [m]
k_a : surface shape factor of crystal
k_v : volumetric shape factor of crystal
L : characteristic size of crystal, m
L_i : mean size of i-th crystal fraction, m
L_m : mean size of crystal population, m
L_{50} : median size of crystals (corresponded to a 50% cumulative weight undersize) [m]
ΔL_i : size range width of i-th crystal fraction [m]
$[LS]_{eq}$: equilibrium concentration (solubility) of L-sorbose [mass%]
$[LS]_{ml}$: concentration of L-sorbose in mother liquor [mass%]
$[LS]_{rm}$: concentration of L-sorbose in a feeding solution [mass%]
M_T : suspension density (mass of crystals per unit volume of suspension) [kg m^{-3}]
m : mass [kg]
m_i : mass of i-th crystal fraction [kg]
n : population density (number of crystals within the defined size range divided by this size range width per unit volume of suspension) [m^{-1} m^{-3}]
n_i : population density of i-th crystal fraction [m^{-1} m^{-3}]
n_0 : population density of nuclei (zero-size crystals) [m^{-1} m^{-3}]
N : agitator's revolution number [s^{-1}]
q_v : volumetric flow rate of crystal suspension [m^3 s^{-1}]
R : correlation coefficient
T : temperature [K]
T_{cr} : temperature of mass crystallization process [K]
T_{eq} : solubility temperature [K]
T_{rm} : temperature of feeding solution [K]
V : volume [m^3]
V_i : volume of the i-th crystal fraction [m^3]
V_t : total volume of a crystallizer [m^3]
V_w : working volume of a crystallizer [m^3]

Greek Letters

ρ : crystal density [kg m^{-3}]
τ : mean residence time of suspension in a crystallizer working volume, defined as V_w/q_v [s]

REFERENCES

1. L. O. Šnajdman, *Proizvodstvo vitaminov*, *Pishch. Prom.*, Moskva (1973).
2. A. Matynia, B. Wierzbowska and Z. Bechtold, *Przem. Chem.*, **76**, 275 (1997) (in Polish).
3. T. Reichstein and A. Grussner, *Helv. Chim. Acta*, **17**, 311 (1934).
4. J. Boudrant, *Enzyme Microb. Tech.*, **12**, 322 (1990).
5. M. Kulchanek, *Adv. Appl. Microbiol.*, **12**, 11 (1970).
6. M. Rosenberg, J. Švitel, I. Rosenbergova and E. Šturdik, *Acta Biotech.*, **35**, 269 (1993).
7. W.-K. Kim, U.-H. Chun, Y.-M. Park, Ch.-H. Kim, E.-S. Choi and S.-K. Rhee, *Process Biochem.*, **29**, 227 (1994).
8. A. Bonomi, E. F. P. Augusto, N. S. Barbosa, M. N. Mattos, L. R. Magossi and A. L. Santos, *J. Biotech.*, **31**, 39 (1993).
9. M. B. Davies, J. Austin and D. A. Partridge, *Vitamin C: Its chemistry and biochemistry*, The Royal Society of Chemistry, Cambridge (1991).
10 A. Matynia, B. Wierzbowska and Z. Bechtold, *Pol. J. Appl. Chem.*, **47**, 31 (2003).
11. B. Wierzbowska, J. Koralewska, K. Piotrowski, A. Matynia and K. Wawrzyniecki, *Proceedings of European congress of chemical engineering*, CD-ROM, No. 2910, Copenhagen (2007).
12. A. Matynia, B. Wierzbowska and Z. Bechtold, *Przem. Chem.*, **76**, 443 (1997) (in Polish).
13. A. Matynia, B. Wierzbowska and Z. Bechtold, *Inz. Ap. Chem.*, **42**(3), 5 (2003) (in Polish).
14. A. Matynia, B. Wierzbowska and Z. Bechtold, *Chem. Proc. Eng.*, **24**(2), 319 (2003) (in Polish).
15. B. Wierzbowska, J. Koralewska, K. Piotrowski and A. Matynia, *Pol. J. Chem. Techn.*, **8**(4), 14 (2006).
16. A. D. Randolph and M. A. Larson, *Theory of particulate processes: analysis and techniques of continuous crystallization*, Academic Press, New York (1988).
17. J. W. Mullin, *Crystallization*, Butterworth-Heinemann, Oxford (1992).
18. Z. Rojkowski and J. Synowiec, *Crystallization and crystallizers*, WNT, Warszawa, (1992) (in Polish).